Results on light dark matter particles with a low threshold CRESST-II detector

A. Gütlein[*1], G. Angloher[2], A. Bento[3], C. Bucci[4], L. Canonica[4], X. Defay[5], A. Erb[5,6], F. v. Feilitzsch[5], N. Ferreiro Iachellini[2], P. Gorla[4], D. Hauff[2], J. Jochum[7], M. Kiefer[2], H. Kluck[1], H. Kraus[8], J.-C. Lanfranchi[5], J. Loebell[7], A. Münster[5], C. Pagliarone[4], F. Petricca[2], W. Potzel[5], F. Pröbst[2], F. Reindl[2], K. Schäffner[3], J. Schieck[1], S. Schönert[5], W. Seidel[2], L. Stodolsky[2], C. Strandhagen[7], R. Strauss[2], A. Tanzke[2], H. H. Trinh Thi[5], C. Türkoğlu[1], M. Uffinger[7], A. Ulrich[5], I. Usherov[7], S. Wawoczny[5], M. Willers[5], M. Wüstrich[2], and A. Zöller[5]

[1]Institut für Hochenergiephysik der Österreichischen Akademie der Wissenschaften, A-1050 Wien, Austria and Atominstitut, Vienna University of Technology, A-1020 Wien, Austria
[2]Max-Planck-Institut für Physik, D-80805 München, Germany
[3]Departamento de Fisica, Universidade de Coimbra, P3004 516 Coimbra, Portugal
[4]INFN, Laboratori Nazionali del Gran Sasso, I-67010 Assergi, Italy
[5]Physik-Department, Technische Universität München, D-85747 Garching, Germany
[6]Walther-Meißner-Institut für Tieftemperaturforschung, D-85748 Garching, Germany
[7]Eberhard-Karls-Universität Tübingen, D-72076 Tübingen, Germany
[8]Department of Physics, University of Oxford, Oxford OX1 3RH, United Kingdom

February 25, 2016

Abstract

The CRESST-II experiment is a direct dark matter search using cryogenic detectors based on scintillating calcium-tungstate crystals. The detectors are operated at millikelvin temperatures and are read out by transition edge sensors. Due to the resulting low energy thresholds and the light nuclei of calcium tungstate, our detectors provide for a high sensitivity for dark-matter particles with low masses.

In this contribution we present the results of a blind analysis of data corresponding to an exposure of $52\,\mathrm{kg}$-days which were obtained during phase 2 of CRESST-II between July 2013 and August 2015. For this analysis only the detector module with the lowest energy threshold of $307\,\mathrm{eV}$ for nuclear recoils is taken into account. The result of this analysis is the best sensitivity for the elastic spin-independent scattering cross section for masses of dark-matter particles below $\sim 2\,\mathrm{GeV/c^2}$. In particular, due to the low threshold we were able to probe new parameter space down to masses of $0.5\,\mathrm{GeV/c^2}$.

1 Introduction

The dynamics of galaxies and galaxy clusters provide several hints for the existence of cold dark matter [1, 2, 3]. From the precise measurements of the temperature fluctuations of the cosmic microwave background we know that $\sim 27\,\%$ of the energy density of the universe is due to dark matter [4]. However, the nature and origin of dark matter remains still unknown. Solving this dark-matter puzzle is one of the major challenges of modern particle physics.

Direct dark matter searches [5, 6, 7, 8, 9, 10, 11, 12, 13, 14, 15] aim at the detection of scatterings of dark matter particles off the nuclei of the detector material. The CRESST-II experiment [7, 16, 17] is using cryogenic bolometers based on calcium tungstate ($CaWO_4$) crystals. These detectors are operated at millikelvin temperatures and are read out by transition edge sensors (TES). The TES is a thin metal film (tungsten for CRESST detectors) which is stabilized at the steep phase transition between normal and superconductivity, hence the operation at millikelvin temperatures. A particle interaction inside a $CaWO_4$ crystal generates

---

*corresponding author (achim.guetlein@oeaw.ac.at)

phonons. The phonons are propagating through the crystal reaching the TES, which is connected to the crystal [16, 17]. These phonons cause a small increase of the temperature of the TES. This leads to a detectable large increase of the electric resistance of the TES due to the steepness of the phase transition. The read out change in resistance is proportional to the energy deposited inside the $CaWO_4$ crystal.

In addition, a small amount of the deposited energy is converted into scintillation light. This light is detected by a separate light detector. The light detectors are cryogenic calorimeters based on silicon or silicon-on-sapphire (SOS) discs. Similarly to the $CaWO_4$ detectors, the light detectors are also equipped with TESs to measure the scintillation light absorbed by silicon or SOS discs. To improve the detection efficiency for scintillation light both detectors are surrounded by a reflective and scintillating housing.

The interactions of incident particles with electrons of $CaWO_4$ lead to a different amount of scintillation light as interactions with nuclei. Thus, it is possible to distinguish between electron and nuclear recoils. Since the majority of the backgrounds interacts with electrons and dark matter particles are expected to interact mainly with nuclei, an efficient background rejection is possible due to the simultaneous measurement of the phonon and scintillation-light signals generated by particle interactions inside $CaWO_4$.

2   Data selection

The dataset used for this contribution was obtained by one detector module operated during phase 2 of CRESST-II between July 2013 and August 2015. In 2014 we were able to change the threshold of this module's $CaWO_4$ detector down to 307 eV [7] which is the lowest threshold of all $CaWO_4$ detectors of the 18 modules operated in CRESST-II, phase 2. Only data with a threshold of 307 eV are taken into account for the blind analysis whose results are presented in this work. This dataset corresponds to an exposure of 51 kg live-days before cuts.

The threshold was determined by so-called test pulses, i.e., the detector response to electrical signals sent to the detectors. The left panel of figure 1 depicts the fraction of test pulses (black dots with binomially distributed
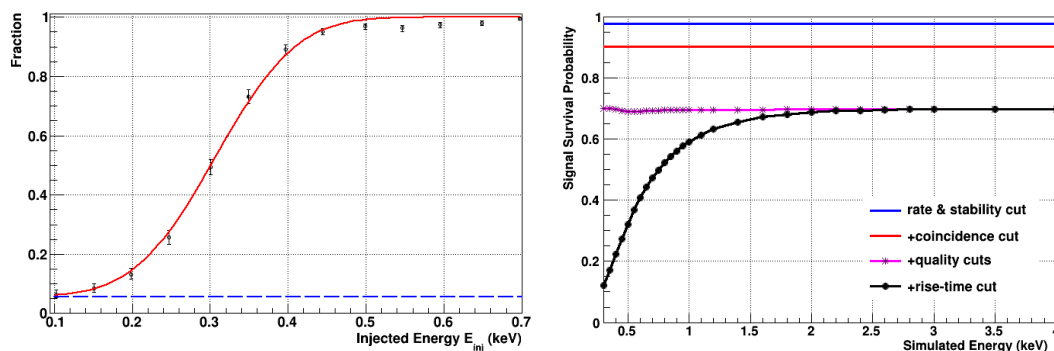

Figure 1: *Left panel*: The fraction of test pulses (black dots, binomially distributed errors) which are triggered by the read-out electronics as a function of the energy injected into the $CaWO_4$ detector. The measured efficiencies are fitted by the red curve composed of a scaled error function and a constant part (dashed blue line) accounting for pile up. The energy (307 eV) where the error function is 50 % of its maximal value is used as threshold.
Right panel: The cumulative signal-survival probabilities for the different cuts applied to the data. The rate and stability cut (blue line) and the coincidence cut (red line) are independent of the energy. The survival probabilities of the energy dependent data-quality cuts (magenta line) and rise-time cut (black line) are determined by applying these cuts to artificial pulses (see text for further details).

errors) which are triggered by the read-out electronics as a function of injected energy. These measured trigger efficiencies are fitted by the red curve composed of a scaled error function and a constant part (dashed blue line) accounting for pile up where the electronic triggers on the sum of a particle event and a test pulse. The energy where the error function is 50 % of its maximal value gives the threshold. For the $CaWO_4$ detector presented in this work we obtained an energy threshold of 307 eV.

The right panel of figure 1 shows the cumulative signal-survival probabilities of the different cuts applied to the data as a function of the energy. The energy independent rate and stability cuts (blue line) remove time periods with abnormal trigger rates and unstable working conditions. The energy independent coincidence cut (red line) removes events which are in coincidence with the muon veto-system or events in other detector modules[1].

---

[1]Due to their small cross section, dark matter particles are expected to interact at maximum with one module. Coincidences with the muon veto are almost always random due to gamma events in the veto. Thus, the coincidence cut is independent of the

The energy dependent data quality cuts (magenta line) and the rise-time cut (black line) remove all events where a correct energy reconstruction is not possible (see [7] for more details). The survival probabilities of these energy dependent cuts were determined by applying the cuts to artificial pulses. These artificial pulses are created by superimposing measured baseline-noise samples with scaled signal-templates representing events with different energies. The signal templates for the $CaWO_4$ detector and the light detector, respectively, are created by averaging measured pulses. After applying all cuts the survival probability is $\sim 10\,\%$ at the energy threshold of $307\,\mathrm{eV}$. As will be shown later, this provides a high sensitivity for low masses of dark-matter particles since the expected recoil energies generated are also very small ($\lesssim 1\,\mathrm{keV}$ for masses $\lesssim 1\,\mathrm{GeV/c^2}$).
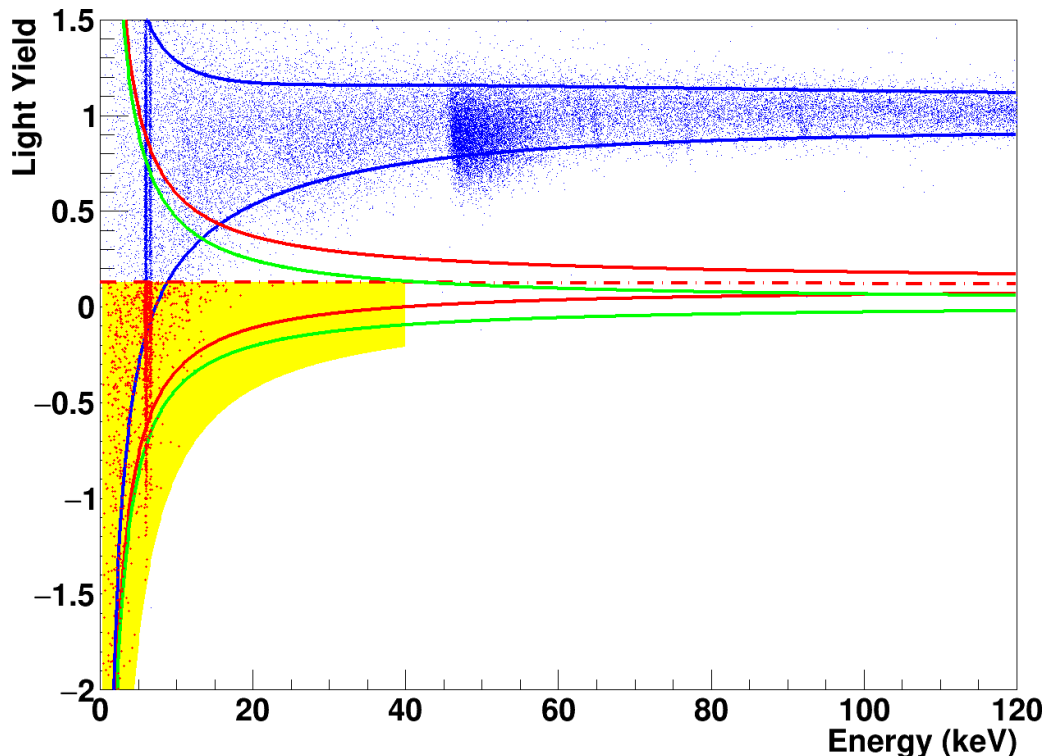

Figure 2: Events surviving all cuts (blue/red dots) on the light yield vs. energy plane. The central $80\,\%$ of the electron (solid blue lines), oxygen (solid red lines), and tungsten-recoil bands (solid green lines) are also shown. The calcium-recoil band is not shown for reasons of clarity. The dashed red line marks the median of the oxygen band and serves also as upper boundary for the region of interest for the dark matter search which is depicted in yellow. The events accepted for the limit calculation are shown as red dots, i.e., the events in the region of interes. See main text for further details.

Figure 2 shows the events surviving all cuts (blue/red dots) on the light yield vs energy plane, where the light yield is the ratio of the measured scintillation light and phonon signal. The blue solid lines mark the central $80\,\%$ of the electron-recoil band, i.e., a region where $80\,\%$ of the electron-recoil events are expected. The red and green solid lines depict the central $80\,\%$ of the oxygen and tungsten-recoil band, respectively. The calcium-recoil band is not shown for reasons of clarity. The region of interest for the dark matter search is depicted by the yellow region. It spreads from the energy threshold of $307\,\mathrm{eV}$ to an energy of $40\,\mathrm{keV}$. For kinematic reasons for the majority of the dark-matter scatterings only recoil energies below $40\,\mathrm{keV}$ are expected. The lower boundary of the region of interest is the $0.5\,\%$ quantile of the tungsten-recoil band, i.e., $99.5\,\%$ of the tungsten-recoil events are expected to be abouve the lower bound. The upper boundary is given by the median of the oxygen band (red dashed line), i.e., $50\,\%$ of the oxygen-recoil events are expected below this line. This choice serves as a compromise between an efficient background suppression and high sensitivity for dark-matter scatterings at low energies. We also studied the influence of this upper boundary on the resulting limit for the cross section and, as a result, the limit does not depend on reasonable choices of this upper boundary [7]. The events inside the region of interest (red dots) are used for the limit calculation.

The two most prominent features in figure 2 are the structure at $\sim 46\,\mathrm{keV}$ caused by an intrinsic contamination of $^{210}\mathrm{Pb}$ and the two X-ray lines at 5.9 and 6.5 keV caused by an accidental irradiation by a $^{55}\mathrm{Fe}$ calibration source. However, the two X-ray lines have no influence on the limit for masses of the dark-matter particles below $\sim 3\,\mathrm{GeV/c^2}$ [7].

energy.

3   Results

As can be seen in figure 2, the majority of the events inside the region of interest are compatible with the electron-recoil band and, thus, are most likely caused by β and γ backgrounds. No hints for a dark-matter signal are present in these data. Thus, we decided to calculate a limit on the elastic spin-independent cross section for dark-matter particles scattering off nucleons. To be conservative we applied Yellin's optimum interval method [18, 19] which does not take into account knowledge about the backgrounds[2].
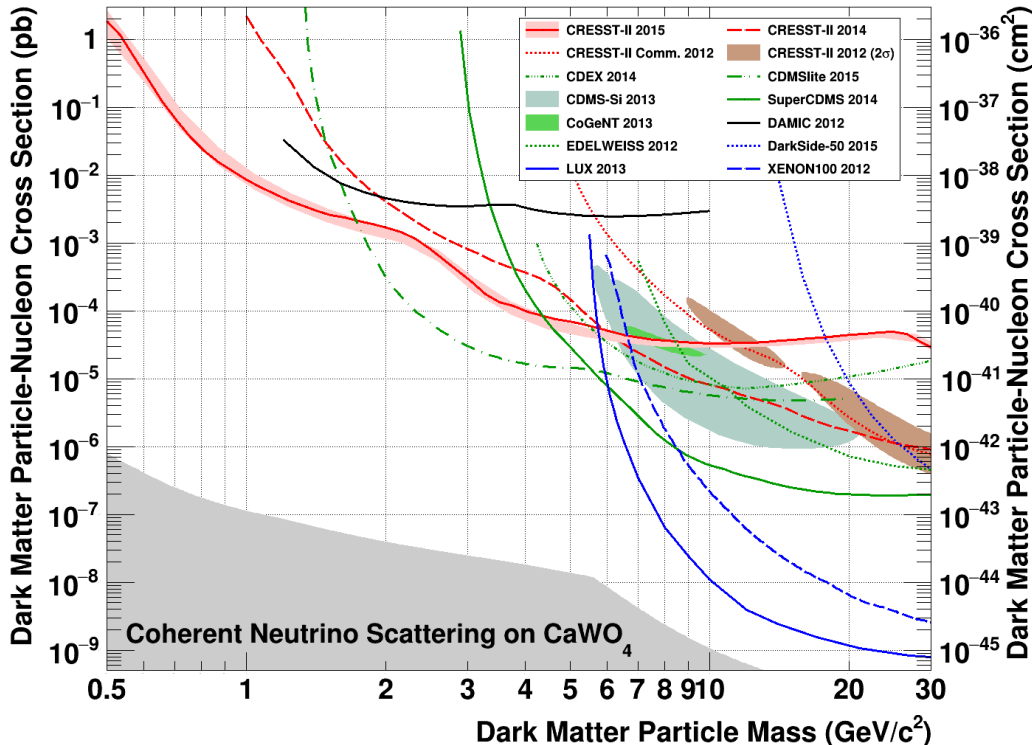

Figure 3: The current results of several direct dark matter searches. The colored regions represent a dark-matter interpretation of excesses over the expected backgrounds of a few experiments. The lines represent the upper limits on the elastic spin-independent scattering cross section as a function of the mass of the dark-matter particles (see main text for further details). The area shaded in grey at the lower left corner depicts the parameter space where solar and atmospheric neutrinos scattering coherently off nuclei are an irreducible background source [20].

Figure 3 shows the current results of several direct dark matter searches. The colored regions represent a dark-matter interpretation of excesses over the expected backgrounds of a few experiments: CDMS-Si (light green) [21], CoGeNT (dark green) [6], and CRESST-II Phase 1 (brown) [22]. However, these dark-matter interpretations are in strong tension with the null results of several other experiments.

The lines represent the upper limits on the elastic spin-independent scattering cross section as a function of the mass of the dark-matter particles. The blue lines are the limits from experiments based on liquid noble gasses: DarkSide (dotted blue) [10], LUX (solid blue) [12], and XENON100 (dashed blue) [15]. The green lines depict the limits from experiments based on germanium as target material: CDEX (dash-dotted line) [5], EDELWEISS (dotted green) [11], SuperCDMS (solid green) [13], and CDMSlite (dashed green) [14]. The limit from the DAMIC experiment [9] using silicon CCDs is depicted as a black solid line. The limits from the CRESST-II experiment using cryogenic bolometers based on $CaWO_4$ are shown as red lines: reanalyzed commissioning run (dotted line) [23], 2014 results based on non-blind analysis of a different module [24] (dashed line), and the result presented in this work as solid red line. The red-shaded region around the solid red line depicts the statistical uncertainties of the limit. These uncertainties are obtained by analysing mock-data sets whose data are distributed following the distribution observed in the measured data set (see, e.g., figure 2) [7]. With this result we are able to explore new parameter space down to masses of dark-matter particles of $0.5\,\mathrm{GeV/c^2}$. For masses below $\sim 2\,\mathrm{GeV/c^2}$ this analysis sets the strongest limit on the cross section for elastic spin-independent scatterings of dark-matter particles off nucleons.

---

[2]In addition, we also chose this method to be compatible with the analysis of our previous results from 2014 [24].

The result of the analysis presented in this work also sets a stronger limit than the result from 2014 [24] for masses below $\sim 6\,\text{GeV/c}^2$. The 2014 result was obtained by the analysis of a non-blind dataset of a different detector module which has a smaller average background rate than the module for the 2015 analysis (~ 3.5 compared to ~ 8.5 events $\text{keV}^{-1}\,\text{kg}^{-1}\,\text{day}^{-1}$ in the energy range of interest). The background rejection is less efficient for the 2015 module compared to the 2014 module due to the performance of the light detector of the 2015 module. However, the energy threshold of the 2015 module ($307\,\text{eV}$) is better than the threshold of the 2014 module ($600\,\text{eV}$). Thus, for the investigation of dark-matter particles with low masses a low energy threshold is more important than low background rates or efficient background rejection.

For low masses, both limits from 2014 and 2015 are limited by detector performance and not by statistics: larger exposures would lead to the same limit.

Taking into account all these results from the comparison of the 2014 and 2015 limits leads to our strategy for the next CRESST-III, where the $CaWO_4$ detectors will be optimized for very low energy thresholds $\lesssim 100\,\text{eV}$ [25]. In particular, the mass of the $CaWO_4$ crystals will be reduced by a factor of 10 to $\sim 25\,\text{g}$ (compared to the 2014 detector) to reach the threshold goal. With such thresholds we could improve the sensitivity on the cross section by about two orders of magnitude with the same background rate as the current detectors.

4   Conclusions and outlook

CRESST-II is a direct dark matter search aiming at the detection of dark-matter particles scattering off the detector material calcium tungstate ($CaWO_4$). In phase 2 of CRESST-II, 18 detector modules were operated between July 2013 and August 2015. The detector modules consist of a $CaWO_4$ detector to measure the energy deposited in the $CaWO_4$ crystal as well as a separate light detector to simultaneously measure the scintillation light generated by a particle interaction in the $CaWO_4$ crystal. Due to different amounts of scintillation light it is possible to distinguish between electron recoils (e.g., β and γ backgrounds) and nuclear recoils. This leads to an efficient rejection of the dominant β/γ backgrounds since dark-matter particles are expected to mainly interact with nuclei.

In this contribution we present the blind analysis of a dataset obtained by one detector module with the best energy threshold of $307\,\text{eV}$ for nuclear recoils. This detector module achieves the best sensitivity for the elastic spin-independent cross section for scatterings of dark-matter particles off nucleons for masses of dark-matter particles below $\sim 2\,\text{GeV/c}^2$. In addition, we are able to probe new parameter space down to masses of $\sim 0.5\,\text{GeV/c}^2$.

A comparison of the 2015 results presented in this work with the 2014 results from an analysis of a different detector module shows that a low energy threshold is more important to achieve a high sensitivity for low masses of dark-matter particles than background rate, efficient background rejection, or large exposures.

These conclusions lead to our strategy of the next phase, CRESST-III, which will start in spring 2016. Our goal is to improve the energy threshold for nuclear recoils to $\lesssim 100\,\text{eV}$. The mass of the $CaWO_4$ crystals will be reduced by a factor of 10 to $\sim 25\,\text{g}$ to reach this threshold goal. Assuming the same average background rate as for the current detectors a threshold of $100\,\text{eV}$ can improve the sensitivity by about two orders of magnitude.

Acknowledgements

References

[1] G. Bertone, et al., Phys. Rept. **405**, 279 (2005)

[2] G. Jungman, et al., Phys. Rept. **267**, 195 (1996)

[3] D. Clowe, et al., Astroph. J. Lett. **648**, L109 (2006)

[4] Planck collaboration: P.A.R. Ade, et al., A&A **571**, A16 (2014), `arXiv:1303.5076`

[5] CDEX collaboration: Q. Yue, et al., Phys. Rev. D **90**, 091701 (2014), `arXiv:1404.4946`

[6] CoGeNT collaboration: C. E. Aslseth, et al., Phys. Rev. D **88**, 012002 (2013), `arXiv:1208.5737`

[7] CRESST collaboration: G. Angloher, et al., Eur. Phys. J. C **76**, 25 (2015), `arXiv:1509.01515`

[8] DAMA collaboration: R. Bernabei, et al., Eur. Phys. J. C **73**, 2648 (2013), `arXiv:1308.5109`

[9] J. Barreto, et al. Phys. Lett. B **711**, 264 (2012), `arXiv:1105.5191`

[10] DarkSide collaboration: P. Agnes, et al., Phys. Lett. B **743**, 456 (2015), `arXiv:1410.0653`

[11] EDELWEISS collaboration: E. Armengaud, et al., Phys. Rev. D **86**, 051701 (2012), `arXiv:1207.1815`

[12] LUX collaboration: D. S. Akerib, et al., Phys. Rev. Lett. **112**(9), 091303 (2014), `arXiv:1310.8214`

[13] SuperCDMS collaboration: R. Agnese, et al., Phys. Rev. Lett. **112**(24), 241302 (2014), `arXiv:1402.7137`

[14] SuperCDMS collaboration: R. Agnese, et al., Phys. Rev. Lett. **116**, 071301 (2016), `arXiv:1509.02448`

[15] XENON100 collaboration: E. Aprile, et al., Phys. Rev. Lett. **109**, 181301 (2012), `arXiv:1207.5988`

[16] CRESST collaboration: G. Angloher, et al., Astropart. Phys. **31**, 270 (2009), `arXiv:0809.1829`

[17] CRESST collaboration: G. Angloher, et al., Astropart. Phys. **23**, 325 (2005), `arXiv:astro-ph/0408006`

[18] S. Yellin, Phys. Rev. D **66**, 032005 (2002), `arXiv:physics/0203002`

[19] S. Yellin, Software for computing an upper limit given unknown background (02/2011) URL `http://cdms.stanford.edu/Upperlimit/`

[20] A. Gütlein, et al., Astropart. Phys. **69**, 44 (2015), `arXiv:1408.2357`

[21] CDMS Collaboration: R. Agnese, et al., Phys. Rev. Lett. **111**, 251301 (2013), `arXiv:1304.4279`

[22] CRESST Collaboration: G. Angloher, et al., Eur. Phys. J. C **72**, 1971 (2012), `arXiv:1109.0702`

[23] A. Brown, et al., Phys. Rev. D **85**, 021301 (2012), `arXiv:1109.2589`

[24] CRESST collaboration: G. Angloher, et al., Eur. Phys. J. C **74**, 3184 (2014), `arXiv:1407.3146`

[25] CRESST collaboration: G. Angloher, et al. `arXiv:1503.08065` (2015)